# Cerium Content and Cycle Life of Multicomponent $AB_5$ Hydride Electrodes

**G. D. Adzic, J. R. Johnson,* J. J. Reilly,* J. McBreen,* and S. Mukerjee***

*Department of Applied Science, Brookhaven National, Laboratory, Upton, New York 11973, USA*

**M. P. Sridhar Kumar,* W. Zhang,** and S. Srinivasan***

*Center for Electrochemical Systems and Hydrogen Research, Texas A&M University, College Station, Texas 77843, USA*

ABSTRACT

Multicomponent $AB_5$ hydrides are attractive replacements for the cadmium electrode in nickel-cadmium batteries. The archetype compound of the $AB_5$ alloy class is $LaNi_5$, but in a typical battery electrode mischmetal is substituted for La and Ni is substituted in part by various metals. While the effects of Ni substitution have been widely studied, relatively little effort has been focused on the effect of La substitution. Cerium is the predominant rare earth in normal mischmetal, and this paper deals with the effect on cycle life and storage capacity due to the increasing presence of Ce in the alloy series $La_{1-x}Ce_xNi_{3.55}Co_{0.75}Mn_{0.4}Al_{0.3}$. Alloys were characterized by the determination of pressure-composition relationships, molar volume of H in the hydride phase and electrode cycle life. The effects due to lattice expansion are taken into account. It was concluded that the rate of loss of electrochemical capacity per charge-discharge cycle due to electrode corrosion was significantly decreased by the presence of Ce.

## Introduction

Multicomponent $AB_5$ hydrides are attractive as replacements for the cadmium electrode in nickel-cadmium batteries from both an environmental and performance viewpoint. However, the paradigm compound of the $AB_5$ class of alloys, $LaNi_5$, is not a suitable electrode because it corrodes rapidly in the chemically aggressive battery environment. This problem can be ameliorated by partial substitution of Ni by various metals such as Co, Al, Si, etc. The efficacy of this remedy has been attributed primarily to the reduction of the molar volume of hydrogen, $V_H$, in the hydride phase thereby reducing alloy expansion and contraction during the charge-discharge cycle. This in turn leads to a reduction of the flushing action of the electrolyte through the small pores and fissures of the alloy produced in the initial activation process. Consequently, corrosion of the electrode is reduced.[1] While the effects of Ni substitution have been widely studied, relatively little effort has focused on the effect of La substitution. This neglect is probably due to the good performance and low cost of mischmetal (Mm), which constitutes the A component in commercial $AB_5$ battery electrodes. The rare-earth composition of mischmetal (Mm) corresponds to that of the ore body from which it is recovered; in bastnasite, the most common ore, it corresponds to (in atom percent, a/o) 50 to 55 Ce, 18 to 28 La, 12 to 18 Nd, 4 to 6 Pr, <0.1 Sm, <2 others. The major component of mischmetal is Ce, and we focus here on the determination of the effect of the substitution of Ce for La on electrode cycle life and storage capacity. In pursuit of this goal we have examined the properties of a homologous series of alloys with a composition corresponding to $La_{1-x}Ce_xNi_{3.55}Co_{0.75}Mn_{0.4}Al_{0.3}$ and measured their comparative performance as battery electrodes. Effects due to lattice expansion and hydride stability were addressed and accounted for. Henceforth, for the sake of brevity, alloys with this $B_5$ composition are written as rare earths $B_5$, *e.g.*, $La_{1-x}Ce_xB_5$. We also compare their performance with $MmB_5$ electrodes.

## Experimental

All the $La_{1-x}Ce_xB_5$ alloys were prepared from high purity, >99.9%, starting components. Mischmetal alloys were prepared using commercial mischmetal. In one case a synthetic mischmetal alloy was prepared using high purity La, Ce, Nd, and Pr. A base line $LaNi_{4.7}Al_{0.3}$ electrode was prepared using a commercial alloy obtained from the Ergenics Corporation, Ringwood, NJ. Except for $LaNi_{4.7}Al_{0.3}$ all the alloys were prepared by arc melting under helium. After the first melt the ingot was inverted and re-melted twice. Each ingot was annealed at 1173 K for ~3 days after which x-ray diffraction (XRD) patterns were obtained for each alloy and lattice parameters determined. Pressure-composition (PC) isotherms were measured for all alloy compositions according to the usual procedure.[2] The molar volume of hydrogen in the hydride phase was determined by preparing the hydride phase via the gas-solid reaction under an $H_2$ pressure of ~10 atm. The reactor was then cooled to 78 K and evacuated. CO was introduced into the reactor and allowed to condense, after which it was slowly warmed to room temperature, venting CO as necessary to avoid excess pressurization. At 298 K the system was vented and the sample removed. This procedure effectively poisoned the alloy surface and prevented hydride decomposition in air for at least several days[3] and permitted XRD patterns of the hydride phase to be obtained in sample holders open to the atmosphere. After poisoning, the alloy hydride was split into three portions; one used in the x-ray procedure and the other two were subjected to hydrogen analyses via thermal decomposition.

Electrodes were fabricated from a portion of each alloy and subjected to electrochemical cycling studies. Each electrode was prepared by mixing −100 mesh alloy particles with a mixture of Teflon suspension and carbon black (Vulcan XC-72) in the weight ratio of 17% Teflon, 33% carbon black, and 50% alloy.[4] The weight of the $AB_5$ intermetallic alloy was 0.075 g. The mixture was then mechanically pressed onto a nickel mesh screen attached to an Ni wire connection which was then sandwiched between two nickel foam (Eltech Corp., Fairport Harbor, OH) disks 1.7 cm in diam. Finally, two Al foil disks were pressed lightly onto each side of the electrode after which the assembled electrode was inserted into a hydraulic press and pressed at 82.7 MPa. The apparent electrode surface area was 4.5 $cm^2$. After pressing, the Al foil was removed by dissolving it in concentrated KOH. The electrode was then introduced into an electrochemical cell containing 6 *m* KOH electrolyte and open to the atmosphere. The counterelectrode was a Pt grid, and the reference electrode was Hg/HgO. The electrode was activated *in situ* via successive electrochemical charge and discharge cycles. The cycle life measurements were carried out using a computer-controlled battery cycler (Arbin Corp., College Station, TX). After activation, the charging rate was kept constant at 15 mA for 2 h, which is approximately equivalent to a rate of 0.66 C. The discharge current was constant at 10 mA (~0.5 C rate); it was cutoff when the anodic voltage decreased to −0.70 V *vs.* the Hg/HgO reference electrode.

* Electrochemical Society Active Member.
** Electrochemical Society Student Member.

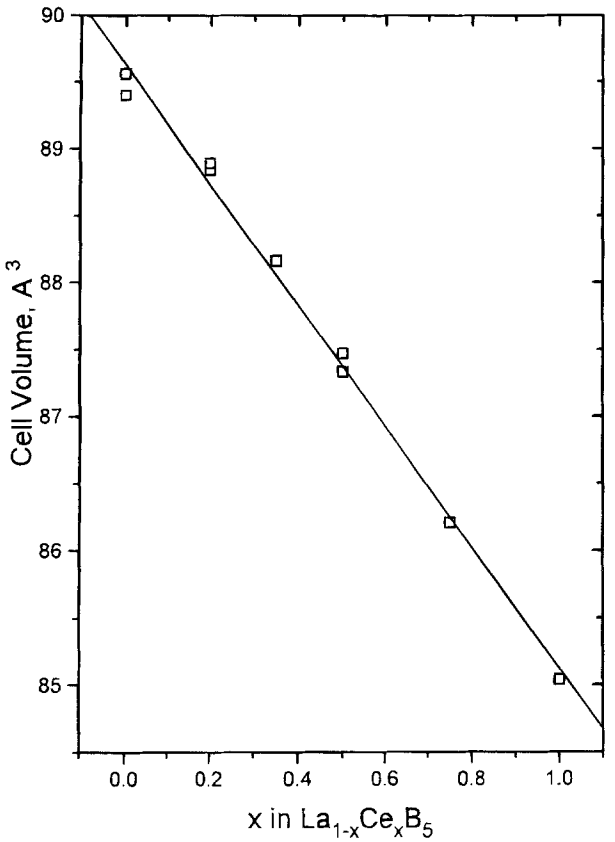


**Fig. 1. Variation of the unit cell volume of $La_{1-x}Ce_xB_5$ with $x$.**

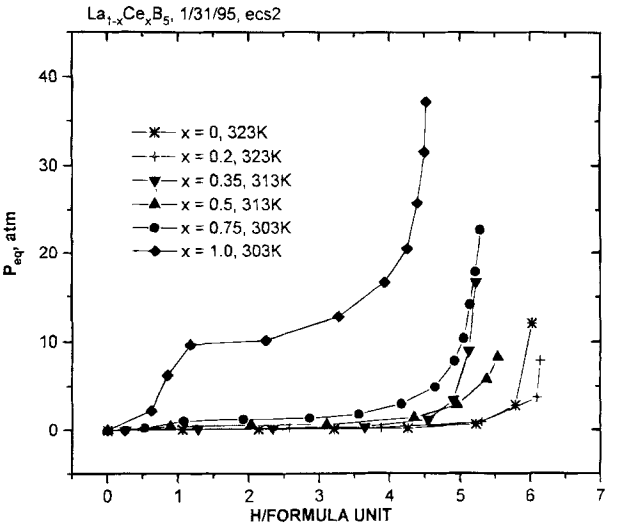


**Fig. 2. PC isotherms of the $La_{1-x}Ce_xB_5$ system; ✳, $x = 0$ (323 K); +, $x = 0.2$ (323 K); ▼, $x = 0.35$ (313 K); ▲, $x = 0.5$ (313 K); ●, $x = 0.75$ (303 K); ◆, $x = 1$ (303 K).**

## Results and Discussion

*X-ray diffraction.*—The variation of the volume of the $AB_5$ unit cell as a function of $x$ in $La_{1-x}Ce_xB_5$ is shown in Fig. 1. The cell volume is of interest because it can be correlated with the stability of the hydride phase in any homologous alloy series.[5] The cell volume is also a linear function of the Ce content and is a useful check on the intermetallic composition. The equation for the cell volume as a function of $x$ is

$$\text{Cell volume} = (-4.5058x + 89.300)\ \text{Å}^3 \qquad [1]$$

The lattice parameters of the starting alloys, their respective hydride phases, and the molar volume of hydrogen, $V_H$, in the latter are listed in Table I. All the samples could be indexed as having hexagonal symmetry and were essentially single phase. For the calculation of $V_H$, the unit cell is assumed to contain one formula unit for both the metal and the hydride phases. $V_H$ is based on the expansion of the hexagonal unit cell per H atom inserted, $n$, *i.e.*

$$V_H = (\text{Vol}_{AB_5H_n} - \text{Vol}_{AB_5})(n^{-1}) \qquad [2]$$

where the units of volume are Å$^3$.

Attention should be called to the low $V_H$ in α-$CeB_5H_n$. The lower value of $V_H$ in the H solid-solution region (α-phase) is not without precedent, *e.g.*, in $LaNi_5H_{0.165}$ $V_H$ is reported[6] to be 2.6 Å$^3$ per H atom whereas in the hydride phase[1] it is 3.5 Å$^3$.

*Pressure composition isotherms.*—PC isotherms for $La_{1-x}Ce_xB_5$ alloys are shown in Fig. 2. There is little hysteresis in the more stable systems ($x < 0.75$), and only absorption isotherms are shown for the sake of clarity.

The maximum H content for $La_{1-x}Ce_xB_5$ is achieved when $x = 0.2$; however at $x > 0.2$ there is a decrease in the H storage capacity and hydride stability until at $x = 1$ the decrease in both stability and storage capacity is marked. This trend is not unexpected as the unit cell volume decreases with Ce content (Fig. 1). It is obvious that the $B_5$ composition greatly influences hydride stability since the

**Table I. Lattice parameters and $V_H$.**

| Composition | Alloy (no.) | $a$ (Å) | $c$ (Å) | Cell Volume (Å$^3$) | $V_H$ (Å$^3$/atom) |
|---|---|---|---|---|---|
| $LaB_5$ | 2040 | 5.0642 | 4.0325 | 89.56 | |
| $LaB_5H_{5.84}$ | 2040 | 5.3911 | 4.2387 | 106.69 | 2.93 |
| $LaB_5$ | 2059 | 5.0615 | 4.0298 | 89.40 | |
| $LaB_5H_{6.01}$ | 2059 | 5.3947 | 4.2681 | 107.77 | 3.05 |
| $La_{0.8}Ce_{0.2}B_5$ | 2036 | 5.038 | 4.0416 | 88.84 | |
| $La_{0.8}Ce_{0.2}B_5H_{5.91}$ | 2036 | 5.3985 | 4.2728 | 107.84 | 3.21 |
| $La_{0.65}Ce_{0.35}B_5$ | 2058 | 5.0168 | 4.0451 | 88.16 | |
| $La_{0.65}Ce_{0.35}B_5H_{5.68}$ | 2058 | 5.3790 | 4.2522 | 106.54 | 3.24 |
| $La_{0.5}Ce_{0.5}B_5$ | 2034 | 4.9934 | 4.0446 | 87.33 | |
| $La_{0.5}Ce_{0.5}B_5H_{5.55}$ | 2034 | 5.353 | 4.2229 | 104.79 | 3.15 |
| $La_{0.25}Ce_{0.75}B_5$ | 2033 | 4.9538 | 4.0559 | 86.19 | |
| $La_{0.25}Ce_{0.75}B_5H_{2.84}$ | 2033 | 5.1546 | 4.1358 | 95.16 | 3.15 |
| $CeB_5$ | 2061 | 4.9226 | 4.0523 | 85.04 | |
| $CeB_5H_{0.62}$ (α-phase) | 2061 | 4.9365 | 4.0766 | 86.03 | 1.60 |
| $MmB_5$ (Synthetic Mm) | 2049 | 4.9890 | 4.0545 | 87.39 | |
| $MmB_5H_{4.60}$ (Synthetic Mm) | 2049 | 5.2945 | 4.1872 | 101.65 | 3.10 |
| $MmB_5$ | 2063 | 4.9626 | 4.0560 | 86.50 | |
| $MmB_5H_{3.12}$ | 2063 | 5.1853 | 4.1335 | 96.25 | 3.13 |
| $MmNi_{3.5}Mn_{0.4}Al_{0.3}Co_{0.75}$ | 2031 | 4.9623 | 4.0456 | 86.27 | |
| $MmNi_{3.5}Mn_{0.4}Al_{0.3}Co_{0.75}H_{3.34}$ | 2031 | 5.209 | 4.1309 | 97.07 | 3.23 |
| $LaNi_{3.5}Mn_{0.4}Al_{0.3}Co_{0.75}$ | 2032 | 5.0699 | 4.0392 | 89.91 | |
| $LaNi_{3.5}Mn_{0.4}Al_{0.3}Co_{0.75}H_{6.11}$ | 2032 | 5.4074 | 4.2743 | 108.23 | 3.00 |
| $LaNi_{4.7}Al_{0.3}$ | | 5.0195 | 4.0076 | 87.44 | |
| $LaNi_{4.7}Al_{0.3}H_{5.30}$ | | 5.3385 | 4.2558 | 105.82 | 3.47 |

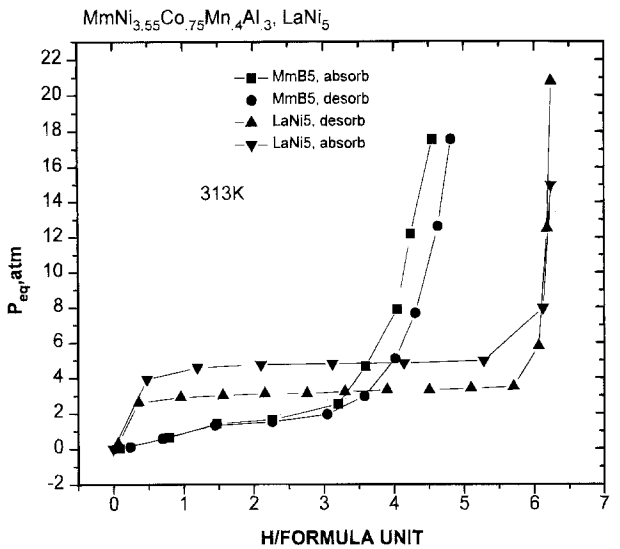


**Fig. 3. PC isotherms for $LaNi_5$ and $MmB_5$; ▲, desorption $LaNi_5$; ▼, absorption $LaNi_5$; ●, desorption $MmB_5$; and ■, absorption $MmB_5$.**

desorption plateau pressure for $CeNi_5H_x$ is reported to be 90 atm at 295 K.[7]

In Fig. 3 we show both absorption and desorption PC isotherms for $MmB_5H_x$ and $LaNi_5H_x$. Only the latter exhibits a significant hysteresis effect. The lack of hysteresis near room temperature in multicomponent $AB_5$ hydrides is not unusual, but it is almost always present in the less complex binary and ternary systems. With one exception ($x$ = 0.2 in $La_{1-x}Ce_xB_5$), all multicomponent alloys have significantly less hydrogen storage capacity than $LaNi_5H_x$. This is the usual consequence of the substitution of Ni and La by other metals.

*Cycle life.*—The cycle life of $La_{1-x}Ce_xB_5$ and $MmB_5$ electrodes is illustrated graphically in Fig. 4 and 5 by plotting the electrochemical discharge capacity, $Q$, *vs.* cycles. Inspection of the individual plots reveals the following general behavior. There is an initial steep increase in capacity in the first few cycles; this comprises the activation process which consists of particle size reduction and surface reconstruction. After activation, a maximum in electrochemical storage capacity, $Q_{max}$, is reached. This is usually followed by an essentially linear decrease in capacity as a function of cycles which may be termed capacity decay. It is defined as the slope of the capacity *vs.* cycle curve, *i.e.*, $-dQ/d$ cycle, and determined via a least squares fit of the data as shown in Fig. 5.

The decreased capacity found in all $La_{1-x}Ce_xB_5$ alloys (Fig. 4) with $x > 0.35$ conforms to the shorter and higher plateau pressures of the isotherms depicted in Fig. 2. The extremely low electrochemical capacity of $CeB_5$ is obviously a consequence of the high instability of the hydride phase. Most cycle experiments were repeated, but only one plot for each composition is shown in Fig. 4. However all the experiments and results are listed in Table II. To confirm the behavior of $LaB_5$ three cycle life experiments were carried out using two separate alloys (electrodes T54, 30, 51). The value for $V_H$ as shown in Table II for $LaB_5$ is the average of the two determinations shown in Table I. In all three experiments capacity decay ($-dQ/d$ cycle) was reproducible and relatively high.

The cycle-life data in Table II are listed in order of increasing capacity decay. Two electrodes $La_{0.25}Ce_{0.75}B_5$ and $MmB_5$ (29 and 24), have been subjected to 300 or more cycles without any significant loss in storage capacity. This is good evidence that the physical integrity of all the electrodes, prepared as described in the Experimental Section, is good and that the decay and corrosion rates listed in Table II and calculated from the plots in Fig. 4 and 5 are due to electrode corrosion and not experimental artifacts.

To determine the effect of Ce substitution, it is necessary to determine lattice expansion quantitatively. Thus Table II lists a new parameter, $\Delta\epsilon$, in addition to the H content, $n$, and capacity decay. $\Delta\epsilon$ is a function of $V_H$ and the H content, here expressed as the number of H atoms, $n$, per formula unit; $n$ is calculated from $Q_{max}$ via the Faraday equation

$$n = 3600(Mw \times Q_{max})(9.65 \times 10^7)^{-1} \quad [3]$$

where $Mw$ is the molecular weight of the alloy and the units of $Q$ are mAh/g. It is assumed that after activation the remaining uncorroded alloy in each subsequent charge-discharge cycle is hydrided and dehydrided to the same degree and $n$ is constant. However, $Q$ is usually not constant since it is a function of the weight of the uncorroded alloy in each cycle. Thus for the unit cell, which contains one formula unit, undergoing the phase-conversion process

$$\Delta\epsilon = V_H n \quad [4]$$

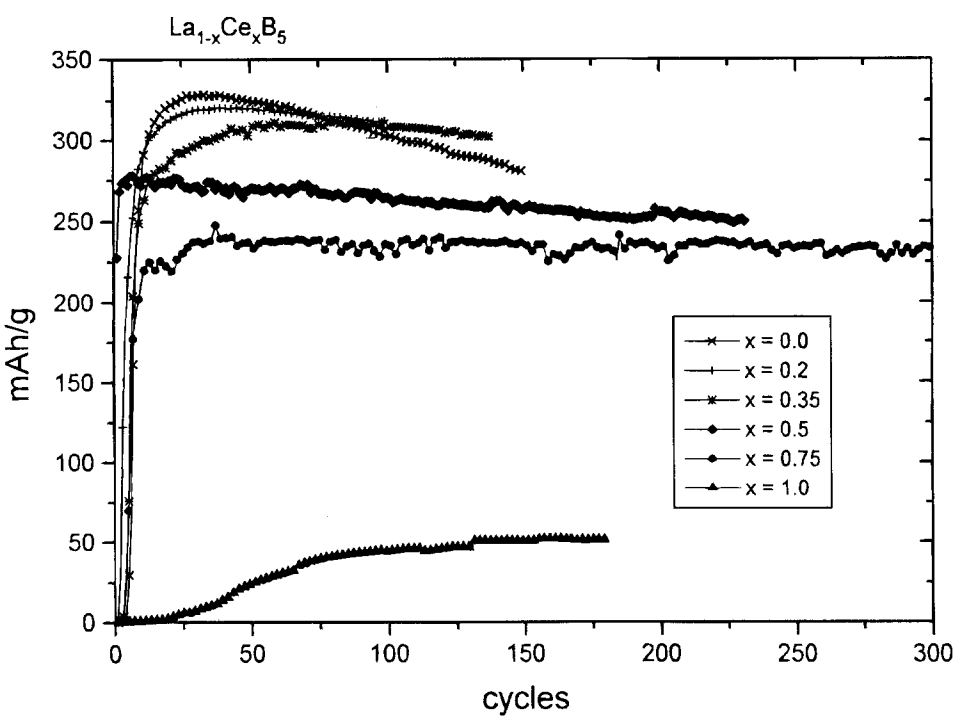


**Fig. 4. Capacity, $Q$, *vs.* charge-discharge cycles for $La_{1-x}Ce_xB_5$ electrodes; ×, $x$ = 0.0; +, $x$ = 0.2; ✳, $x$ = 0.35; ◆, $x$ = 0.5; ●, $x$ = 0.75; and ▲, $x$ = 1.0. Only every third datum point is shown.**

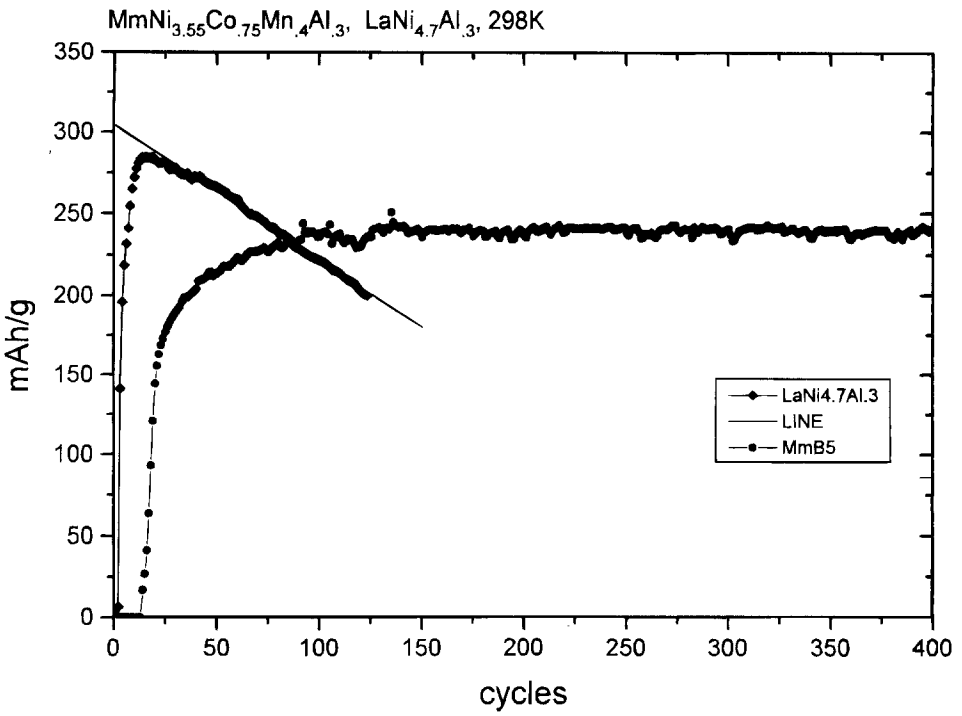


**Fig. 5. Capacity, *Q*, *vs.* charge-discharge cycles for two electrodes, ●, $MmB_5$ and ◆, $LaNi_{4.7}Al_{0.3}$. A linear least squares line is shown for the latter plot.**

where $\Delta\epsilon$ is the actual volume change of the unit cell in Å$^3$ in each charge or discharge cycle.

In the series $La_{1-x}Ce_xB_5$, the greatest values of $\Delta\epsilon$ correspond to compositions where $x$ = 0.2 and 0.35 (electrodes 47,T50, 26); yet the capacity decay for these alloys is significantly less than that for the unsubstituted alloys (electrodes 30, 51, T54). It is not at all surprising that the decay rate is very low for $x$ = 0.75 (no. 29) because it absorbs significantly less hydrogen than the samples with reduced Ce content and, therefore, $\Delta\epsilon$ is low.

The normal $MmB_5$ electrodes (no. 24, 21-2) have a very low decay rate, but they also have a lower capacity and low $\Delta\epsilon$. The synthetic $MmB_5$ electrodes (no. 27, 46) have a higher storage capacity than the normal Mm electrodes and, since $V_H$ is about the same, a higher $\Delta\epsilon$ and decay rate. However, at present it is not possible to discriminate between $\Delta\epsilon$ or the composition of the A component as the cause of the higher decay rate of the synthetic Mm alloy.

The behavior of the $CeB_5$ electrode (no. 36) is instructive. It has very low capacity because of the instability of the hydride phase as shown in Fig. 2. The low decay rate is due to low storage capacity and a very low $\Delta\epsilon$. Thus the rate of fracturing of the intermetallic is greatly reduced because $\Delta\epsilon$ is very small. Consequently the rate of surface area increase per cycle is diminished, and the activation process is retarded. As shown in Fig. 4, $Q_{max}$ for this electrode was not reached until it was subjected to ~100 cycles. Unfortunately, it was not possible to measure $V_H$ in the hydride phase because it was too unstable and lost $H_2$ when it was subjected to XRD.

The $LaNi_{4.7}Al_{0.3}$ electrode (no. 11) was used as a base line comparison with the more complicated alloy electrodes discussed herein. This relatively simple intermetallic forms a hydride phase somewhat more stable than $LaNi_5$ with a slightly reduced H content.[8] Even though $\Delta\epsilon$ is less than several of the other more complex electrodes, the decay rate is the highest measured. This again illustrates the point that $\Delta\epsilon$ is not the sole criterion of electrode corrosion but that composition also plays an important role; in this case the deciding factor is the $B_5$ composition (compare $LaNi_{4.7}Al_{0.3}$ and $LaB_5$ electrodes). We have included in Table II a calculated $\Delta\epsilon$ of 21 Å$^3$/unit cell for $LaNi_5$ from data abstracted from Willems and Buschow;[1] it exceeds that for any other alloy by a large margin. Consequently, it is not surprising that an $LaNi_5H_x$ electrode is reported to have a very high decay rate.[1]

*Alloy corrosion.*—The corrosion of $AB_5$ electrodes has been proposed to occur via the irreversible oxidation of the alloy to form rare-earth hydroxides. For a cycled $LaNi_5$ electrode, it was determined by transmission electron spectroscopy that $La(OH)_3$ was present after cycling.[1] In the present instance an $La_{0.8}Ce_{0.2}B_5$ electrode subjected to 700 charge-discharge cycles contained $La(OH)_3$, $Ce(OH)_3$, and Ni metal as determined by XRD. The presence of rare-earth hydroxides, Ni, and nickel oxides has been reported in electrochemically cycled $AB_5$ electrodes as determined by x-ray absorption near-edge structure (XANES)[9] and x-ray photoelectron spectroscopy (XPS) studies.[10] Thus the loss of electrochemical capacity is directly proportional to the loss of the $AB_5$ alloy by oxidation and readily calculated as follows

$$\frac{d[AB_5]}{d\ \text{cycle}} = \left(\frac{-dQ}{d\ \text{cycle}}\right)(Q_{max})^{-1} \times 100 \qquad [5]$$

where the units of $AB_5$ are in mole percent. This equation is valid provided that the physical integrity of the electrode is maintained. The corrosion rate for all alloys, in units of mol %/cycle, is given in Table II. The effect of Ce content on electrode corrosion is clearly shown in Fig. 6, which illustrates plots of alloy corrosion and $\Delta\epsilon$ *vs.* Ce content for all the $La_{1-x}Ce_xB_5$ electrodes (data for electrode T47 is included despite the slightly reduced Ni content). There is a precipitous decrease in alloy corrosion rate between $x$ = 0 and 0.2 despite the fact that $\Delta\epsilon$ actually increases slightly. On the basis of lattice volume change one would predict a slight increase in corrosion. On further increase in Ce content the corrosion rate again can be correlated to $\Delta\epsilon$. The results are clear and unequivocal; the presence of a relatively small amount of Ce can greatly reduce corrosion even though $\Delta\epsilon$ may be unchanged or even increased.

## Conclusion

From the above considerations we have concluded that corrosion and the consequent decay in storage capacity of $La_{1-x}Ce_xB_5$ electrodes is not solely a function of the volume change per cycle, $\Delta\epsilon$, but also rare-earth composition. The presence of a small amount of cerium has been shown to retard corrosion regardless of lattice expansion/contraction due to hydride formation/decomposition. A possible explanation for this finding lies in that Ce can form a protective oxide film on metal surfaces (Al, mild steel, and others) and it has been shown via XANES studies that Ce

**Table II. Cycle life of modified $AB_5$ Electrodes $B_5 = Ni_{3.55}Co_{0.75}Mn_{0.4}Al_{0.3}$.**

| Electrode | Mw | Electrode (no.) | $V_H$ (Å³/atom) | $n$ (H atoms/unit cell) | $\Delta\epsilon$ (Å³/unit cell) | Cycles | $Q_{max}$ (mAh/g) | Decay $dQ/d$ cycle (mAh/g · c) | Alloy corrosion mol %/cycle |
|---|---|---|---|---|---|---|---|---|---|
| $CeB_5$ | 422 | 36 | 1.60 | 0.8 | 1.3 | 180 | 51 | 0.0 | 0.0 |
| $MmB_5$ | 422 | 24 | 3.13 | 3.9 | 12.2 | 400 | 247 | 0.004 | 0.002 |
| $La_{0.25}Ce_{0.75}B_5$ | 422 | 29 | 3.15 | 3.8 | 12.0 | 300 | 241 | 0.015 | 0.003 |
| $MmNi_{3.50}Mn_{0.4}Al_{0.3}Co_{0.75}$ | 420 | 21-2 | 3.23 | 3.6 | 11.6 | 140 | 230 | 0.041 | 0.018 |
| $La_{0.5}Ce_{0.5}B_5$ | 422 | T49 | 3.15 | 4.4 | 13.9 | 230 | 278 | 0.11 | 0.040 |
| $La_{0.8}Ce_{0.2}B_5$ | 421 | 58 | 3.21 | 4.8 | 15.4 | 130 | 305 | 0.13 | 0.042 |
| $La_{0.8}Ce_{0.2}B_5$ | 421 | 6 | 3.21 | 4.6 | 14.7 | 92 | 293 | 0.14 | 0.047 |
| $La_{0.5}Ce_{0.5}B_5$ | 422 | 32 | 3.15 | 4 | 12.8 | 275 | 260 | 0.14 | 0.054 |
| $La_{0.8}Ce_{0.2}B_5$ | 421 | 37 | 3.21 | 4.6 | 14.8 | 190 | 293 | 0.15 | 0.051 |
| $La_{0.8}Ce_{0.2}B_5$ | 421 | T50 | 3.21 | 5.0 | 16.1 | 80 | 318 | 0.18 | 0.057 |
| $La_{0.65}Ce_{0.35}B_5$ | 422 | 26 | 3.24 | 5.0 | 16.2 | 303 | 318 | 0.18 | 0.057 |
| $MmB_5$ (synthetic) | 423 | 46 | 3.10 | 4.4 | 13.7 | 130 | 279 | 0.19 | 0.068 |
| $La_{0.8}Ce_{0.2}B_5$ | 422 | 47 | 3.21 | 5.0 | 16.1 | 150 | 318 | 0.21 | 0.066 |
| $MmB_5$ (synthetic) | 423 | 27 | 3.10 | 4.3 | 13.3 | 200 | 273 | 0.26 | 0.095 |
| $LaNi_{3.50}Mn_{0.4}Al_{0.3}Co_{0.75}$ | 420 | T47 | 3.23 | 4.9 | 14.7 | 140 | 313 | 0.41 | 0.130 |
| $LaB_5$ | 421 | T54 | 2.99 | 4.8 | 14.3 | 75 | 305 | 0.46 | 0.150 |
| $LaB_5$ | 421 | 51 | 2.99 | 5.2 | 15.5 | 150 | 331 | 0.46 | 0.139 |
| $LaB_5$ | 421 | 30 | 2.99 | 5.1 | 15.2 | 125 | 325 | 0.47 | 0.145 |
| $LaNi_{4.7}Al_{0.3}$ | 423 | 11 | 3.47 | 4.5 | 15.6 | 125 | 285 | 0.83 | 0.291 |
| $LaNi_5$ (Ref. 1) | | — | 3.5 | 6.0 | 21.0 | — | 372 | 45% loss 100 cycle | |

in the film is present as four-valent $CeO_2$.[11] Recent work has reported that Ce in the unhydrided bulk alloy of $La_{0.8}Ce_{0.2}Ni_{4.8}Sn_{0.2}$ is present as a four-valent atom.[9]

We note further that, although the $MmB_5$ electrode has only a modest storage capacity, such electrodes are useful because of their extended lifetime (possibly due to the formation of a protective coating of $CeO_2$ on the alloy surface). However, a battery incorporating an $La_{1-x}Ce_xB_5$ electrode with $x = 0.2$ would have a better overall performance than one with a normal $MmB_5$ electrode although it would be more costly. A more practical alternative may be to use mischmetal with reduced Ce content, *e.g.*, ~20 a/o, for battery electrodes; this would tend to increase storage capacity without sacrificing corrosion resistance. In this connection we point out that two other major components of mischmetal, Pr and Nd, may also form four-valent oxides and both have been reported to form protective oxide films.[12] Finally, if the reduced corrosion attributed to the presence of Ce is due to a mechanism involving the surface formation of $CeO_2$, then its inclusion in other types of metal hydride electrodes may have a similar beneficial effect.

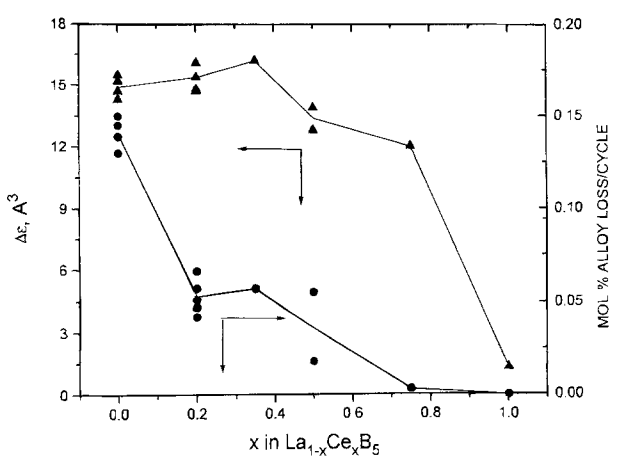


**Fig. 6. ▲, Δε, and ●, alloy corrosion (m/o/cycle); the solid line is drawn through the average *Y* value when more than one *Y* value is given.**

## Acknowledgment

This work was supported by the Chemical Sciences Division, Office of Basic Energy Sciences, U.S. Department of Energy, under Contract No. DE-AC02-76CH00016 and DE-FG03-93ER14381.

Manuscript submitted March 17, 1995; revised manuscript received May 25, 1995.

*Brookhaven National Laboratory assisted in meeting the publication costs of this article.*

REFERENCES

1. J. J. G. Willems and K. H. J. Buschow, *J. Less-Common Met.*, **129,** 13 (1987).
2. J. J. Reilly and R. H. Wiswall, *Inorg. Chem.*, **13,** 218 (1974).
3. J. R. Johnson and J. J. Reilly, *ibid.*, **17,** 3103 (1978).
4. K. Petrov, A. A. Rostami, A. Visintin, and S. Srinivasan, *This Journal,* **141,** 1747 (1994).
5. D. N. Gruen, M. H. Mendelsohn, and A. E. Dwight, *J. Less-Common Met.*, **56,** 19 (1977).
6. J. F. Lynch and J. J. Reilly, *ibid.*, **87,** 225 (1982).
7. S. N. Klyamkin, and V. N. Verbetsky, *J. Alloys Compounds,* **194,** 41 (1992).
8. M. Mendelsohn, D. M. Gruen, and A. E. Dwight, *J. Less-Common Met.*, **63,** 193 (1979).
9. S. Mukerjee, J. McBreen, J. J. Reilly, J. R. Johnson, G. Adzic, K. Petrov, M. P. S. Kumar, W. Zhang, and S. Srinivasan, *This Journal,* **142,** 2278 (1995).
10. F. Meli, A. Zuettel, and L. Schlapbach, *J. Alloys Compounds,* **190,** 17 (1992).
11. A. J. Davenport, H. S. Isaacs, and M. W. Kendig, *Corros. Sci.*, **32,** 653 (1991).
12. D. R. Arnott, B. R. W. Hinton, and N . E. Ryan, *Corrosion,* **45,** 12(1989).